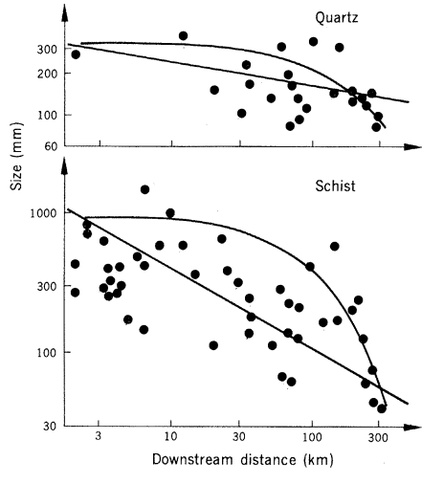

Fig. 2 (left). Log-log diagrams (with normal values) showing same data as in Fig. 1. Curved lines are those that are straight in Fig. 1 and correspond to a constant coefficient for the pebbles; new straight lines, drawn in by eye, represent coefficients that decrease with distance from source.

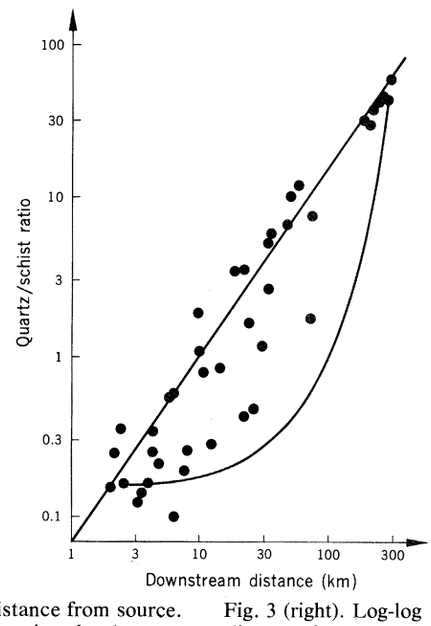

Fig. 3 (right). Log-log diagram with data points and eye-fitted line showing the downstream distance from source increase in the proportion of quartz to schist. About 40 streams and rivers are represented. The curved line corresponds to a constant value for α_P, and the straight line to a coefficient that decreases with distance.

proportional change for quartz and schist can be calculated from their point coefficients

$$\alpha_P = 3(\alpha_{Dq} - \alpha_{Ds})$$

$$\alpha_P = 3\left(\frac{0.171}{x} - \frac{0.574}{x}\right) = -\frac{1.21}{x}\ \text{km}^{-1}$$

Figure 3 shows the downstream increase in the weight ratio of quartz to schist gravel. At source the quartz veins are about 5 percent of the bedrock; at Balclutha, 290 km downstream, quartz gravel is 55 times as abundant as schist gravel. Many of the data points are below the line because not all of the schist comes from the furthermost headwater. From the slope of the straight line in Fig. 3, the point and interval coefficients of proportional change are

$$\alpha_P = -\frac{1.17}{x}\ \text{km}^{-1}$$

$$\bar{\alpha}_P = \frac{-1.17 \log_e(294/2)}{294 - 2} = -0.020\ \text{km}^{-1}$$

The point coefficient so determined is in excellent agreement (within 4 percent) with the corresponding value calculated from independent data on the change in size of the largest quartz and schist pebbles. A coefficient of proportional change that decreases with distance ($\alpha_P = -1.17/x\ \text{km}^{-1}$) fits the data points on Fig. 3 much better than the constant value ($\bar{\alpha}_P = -0.020\ \text{km}^{-1}$) that would be predicted if the size change of the quartz and the schist pebbles fitted the Sternberg law rather than the one proposed here.

There is little possibility that the size changes discussed here are caused by a hydraulic selection (*2*) mechanism in which the largest pebbles accumulate in the river headwaters. Erosion rates in the headwaters of the Clutha catchment are so rapid that if pebbles of a particular size were to accumulate they would be conspicuous. No such accumulation is observed, many rivers being in bedrock gorges, and all pebbles must therefore be moved downriver. Again, if selection were important, the downstream size changes—schist initially larger than quartz, then vice versa—would preclude any simple relation between their weight ratio such as that shown in Fig. 3.

The downstream size reduction is therefore mainly due to the abrasive processes of wear, chipping, and fracture. In river headwaters abrasion is initially rapid as the weakest parts of the pebble are preferentially abraded, sharp corners are rounded, and fracture occurs along planes of weakness. Eventually all differences in lithology and weaknesses are removed, and the result is a homogenous, sound pebble, the downstream change of which is well described by the Sternberg law. Pebble abrasion, when allowance is made for wear of unsound pebbles, thus accounts for the downstream changes observed in the Clutha catchment.

JOHN ADAMS
Department of Geological Sciences, Cornell University, Ithaca, New York 14853

References and Notes

1. H. Blatt, G. Middleton, R. Murray, *Origin of Sedimentary Rocks* (Prentice-Hall, Englewood Cliffs, N.J., 1972), p. 59.
2. F. J. Pettijohn, *Sedimentary Rocks* (Harper & Row, New York, ed. 3, 1975), pp. 45–48.
3. I thank H. W. Wellman and other members of the Geology Department, Victoria University, Wellington, New Zealand, where this work was done, for their criticism. Department of Geological Sciences, Cornell University, Contribution No. 633.

25 August 1978

Molecular Structure of an Unusual Organoactinide Hydride Complex Determined Solely by Neutron Diffraction

Abstract. *The structure of an unusual organometallic complex,* $\{Th[(CH_3)_5C_5]_2 H(\mu\text{-}H)\}_2 \cdot C_6H_5CH_3$, *has been determined from neutron diffraction data, using only the direct-methods program MULTAN. Besides providing accurate metrical information on the first organometallic actinide hydride complex, these results have general and far-reaching implications concerning the complexity and size of crystal structures that can be elucidated solely on the basis of neutron diffraction data.*

A common misconception regarding neutron crystallography is that preliminary structural solutions can only be derived after the tedious collection of redundant x-ray data. In spite of the great recent advances in the use of direct methods for phase determination of x-ray diffraction data (*1*), there has been some question about the general applicability of these techniques to neutron data. In the theory of direct methods, as developed for the x-ray case, it is assumed that the scattering amplitudes all have the same (positive) sign, but for neutron diffraction many atoms have negative coherent scattering lengths (b) (*2*); for example, $b_H = -0.374$, $b_{Li} = -0.214$, $b_{Ti} = -0.34$, and $b_{Mn} = -0.39$ (all in units of 10^{-12} cm). Sikka (*3*) estimated that the negative scattering amplitude of hydrogen would be the major limiting factor in applying the symbolic addition procedure for centrosymmetric crystals (where the sign of the structure factor F_{hkl} is + or −). He predicted that if the quantity $\Sigma b_H^2/\Sigma b^2_{all}$ exceeds 25 percent and if there are more than 100 atoms in the unit cell, the structure probably cannot be derived directly from neutron diffraction data. Although

0036-8075/79/0112-0172$00.50/0

the difficulty in such cases may be circumvented by chemically substituting deuterium for hydrogen ($b_D = 0.66 \times 10^{-12}$ cm) or by using the "squared structure" approach of Karle (*4*), it is unlikely that this is necessary. In fact, the relatively small variation of neutron scattering amplitudes (in contrast to the x-ray case, where heavy atoms may dominate the scattering) is an advantage as it partly compensates for the complication of a negative amplitude for hydrogen (*5*, *6*). In the present rather extreme example, the structure of $\{Th[(CH_3)_5C_5]_2H(\mu\text{-}H)\}_2 \cdot C_6H_5CH_3$ was solved with the direct-methods program MULTAN (*7*), using neutron diffraction data. The solution was facile, even though there are 484 atoms per unit cell, 60 percent of which are hydrogen ($\Sigma b_H^2/\Sigma b^2_{all} = 0.31$) and the diffraction data used in the solution extended only to $(\sin\theta)/\lambda = 0.455$ Å^{-1}, where θ is the Bragg angle and λ is the wavelength. These results have general and far-reaching implications concerning the complexity of crystal structures that can be elucidated solely on the basis of neutron diffraction data.

This work also represents the first structural study of an organometallic actinide hydride complex. Molecular compounds with metal-hydrogen bonds are a ubiquitous feature of contemporary organometallic chemistry and play an important role in catalysis and in stoichiometric synthesis (*8*–*12*). Despite this widespread occurrence, metal hydride complexes were not known for the actinide elements, and there was even some question about whether such species could be isolated (*13*). As part of their chemical exploration of actinide organometallic chemistry (*14*–*16*), Manriquez *et al.* (*17*) recently synthesized molecular compounds of thorium and uranium that contain metal-bound hydrogen atoms. Since the ultimate structural characterization of such heavy-element molecules must rest on single-crystal neutron diffraction experiments (*18*, *19*), we undertook the study reported here.

Crystals of the thorium complex $\{Th[(CH_3)_5C_5]_2H(\mu\text{-}H)\}_2 \cdot C_6H_5CH_3$ are monoclinic (space group $P2_1/c$) with four thorium dimers and four toluene molecules per unit cell. The refined cell constants are $a = 27.988(8)$ Å, $b = 9.967(4)$ Å, $c = 17.364(3)$ Å, $\beta = 103.09(1)°$, and volume $V = 4448.0$ Å^3. Intensity data for the 6575 unique reflections to the $(\sin\theta)/\lambda$ limit of 0.565 Å^{-1} were collected with the automatic diffractometer at the Oak Ridge High Flux Isotope Reactor ($\lambda = 1.016$ Å).

After the usual preliminary data processing, normalized structure factors (E's) were calculated by MULTAN and scaled according to parity class for the 3801 unique reflections with a maximum $(\sin\theta)/\lambda$ of 0.455 Å^{-1}. The resulting intensity distribution of E's closely corresponded to the theoretical distribution for a centrosymmetric structure. For the 400 largest E's, with values ranging from 1.58 to 4.53, 2000 phase relationships were generated by the program MULTAN. Eight reflections were automatically chosen as the starting set for the tangent refinement: one "known" reflection [from the Σ_1 results (*3*), its sign was determined to be negative with a probability of > .99], three origin-fixing reflections, and four other reflections that were allowed to have the 16 possible combinations of positive and negative signs.

The 54 highest peaks from an E map, based on the solution with the highest combined figure of merit, included all 42 nonhydrogen atoms in the dimer. Positions of the hydrogen atoms were obtained from successive Fourier maps and least-squares refinements. At this stage it was discovered from a difference Fourier map that the asymmetric unit contains two independent toluene molecules of crystallization in disorder about two independent centers of symmetry. It is of interest to note that many of the previously unassigned peaks in the initial E map can be assigned to toluene carbon positions, and all but one of the top 48 peaks correspond to either thorium or carbon atomic positions.

At the present stage of the refinement, with anisotropic thermal parameters for the two thorium atoms and the four metal-coordinated hydrogen atoms, and with isotropic thermal parameters for all other atoms, residuals are $R(F_0) = 0.194$, $R(F_0^2) = 0.243$, and $R_w(F_0) = 0.230$ for the 3727 data with $F_0^2 \geq \sigma(F_0^2)$ (σ is the estimated standard deviation). Because of the large number of parameters in this problem, it is not possible to treat all atoms anisotropically without lowering the data-to-parameter ratio to an unreasonable value. The high residuals are due mainly to the anisotropic thermal motion of the atoms that are treated only isotropically. However, the correctness of the structural model is indicated by the fact that a final difference Fourier map is virtually featureless.

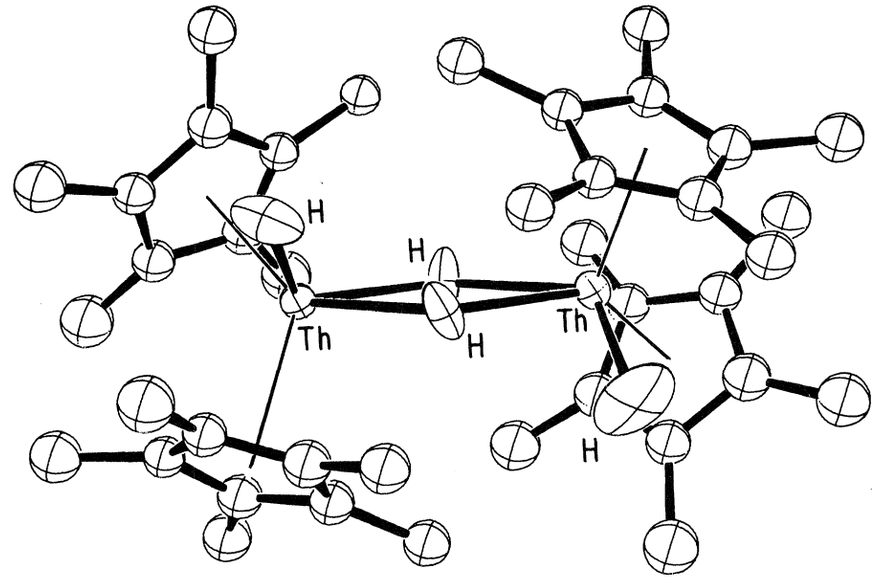

Fig. 1. Perspective view of the $\{Th[(CH_3)_5C_5]_2H(\mu\text{-}H)\}_2$ dimer as determined by single-crystal neutron diffraction. For clarity, hydrogen atoms on the four pentamethylcyclopentadienyl ligands are not included.

The geometry of the $\{Th[(CH_3)_5C_5]_2H(\mu\text{-}H)\}_2$ dimer is shown in Fig. 1. The overall structure can be viewed as two distorted square pyramids sharing a common basal edge. In each half of the dimer, one pentamethylcyclopentadienyl ring occupies the axial vertex and the other ring and the three hydride ligands occupy the four basal vertices. The two thorium atoms and two bridging hydrogen atoms are nearly coplanar. The H-Th-H and Th-H-Th angles are highly acute [average, 58(1)°] and obtuse [average, 122(4)°], respectively.

The separation between the two metal atoms is 4.007(8) Å. Since this distance is considerably longer than the 3.59 Å (*20*) observed in thorium metal, any direct metal-metal interaction in the dimer is probably weak. In the binary hydrides ThH_2 (*21*) and Th_4H_{15} (*22*), where the shortest Th-Th distances range from 3.83 to 4.10 Å, Zachariasen (*22*) attributed the

main cohesive energy to the thorium-hydrogen bonds.

The mean Th-H (terminal) and Th-H (bridging) bond distances in the dimer are 2.03(1) and 2.29(3) Å, respectively. The first value is close to the sum of covalent radii for hydrogen (0.30 Å) and thorium (1.79 Å, assumed equal to the metallic radius), and the second value is ~0.2 Å longer, as found for bridging hydrogen atoms in other transition metal complexes (*23*). For comparison, the thorium-hydrogen bonding distances in ThH_2 and Th_4H_{15} range from 2.29 to 2.46 Å. These longer distances can be attributed to the fact that the hydrogen atoms are more highly coordinated in the binary hydrides (three- and four-coordinated) than in the dimer (one- and two-coordinated).

Other important mean distances and angles in the structure are Th-C (ring), 2.83(1) Å; C (ring)-C (ring), 1.43(1) Å; C (ring)-C (methyl), 1.50(1) Å; C-H, 1.05(1) Å; and $(CH_3)_5C_5$ (centroid)-Th-$(CH_3)_5C_5$ (centroid), 130(1)°. Details of the structure will be published elsewhere (*24*).

Although this is the largest structural problem we have solved to date, we are routinely solving the structures of other organometallic compounds by direct methods with neutron diffraction data. Furthermore, the structural solution of the organic compound melampodin, which is noncentrosymmetric ($P2_12_12_1$) and contains 216 atoms per unit cell ($\Sigma b_H^2/\Sigma b^2_{all} = 0.219$), has been successfully obtained by application of the MULTAN computer program to neutron diffraction data (*25*). Thus we conclude that even for very large hydrogen-containing molecules, direct methods are a very powerful tool for solving structures in neutron diffraction studies.

ROBERT W. BROACH
ARTHUR J. SCHULTZ
JACK M. WILLIAMS
Chemistry Division, Argonne National Laboratory, Argonne, Illinois 60439
GEORGE M. BROWN
Chemistry Division, Oak Ridge National Laboratory, Oak Ridge, Tennessee 37830
JUAN M. MANRIQUEZ
PAUL J. FAGAN, TOBIN J. MARKS
Department of Chemistry, Northwestern University, Evanston, Illinois 60201

References and Notes

1. S. E. Hull, *Acta Crystallogr. Sect. A* **34**, 38 (1978); P. Main, *ibid.*, p. 31; ; M. M. Woolfson, *ibid.* **33**, 219 (1977).
2. G. E. Bacon, *ibid.* **28**, 357 (1972).
3. S. K. Sikka, *ibid.* **25**, 539 (1969).
4. J. Karle, *Acta Crystallogr.* **20**, 881 (1966).
5. J. J. Verbist, M. S. Lehmann, T. F. Koetzle, W. C. Hamilton, *Nature (London)* **235**, 328 (1972).
6. For a discussion of the use of direct methods in neutron diffraction, see G. E. Bacon, *Neutron Scattering in Chemistry* (Butterworths, Boston, Mass., 1977), p. 69.
7. P. Main, M. M. Woolfson, L. Lessinger, G. Germain, J. P. Declercq, "MULTAN 74, A System of Computer Programs for the Automatic Solution of Crystal Structures from X-ray Diffraction Data," Universities of York, England, and Louvain, Belgium (1974); see also J. P. Declercq, G. Germain, P. Main, M. M. Woolfson, *Acta Crystallogr. Sect. A* **29**, 231 (1973).
8. J. C. Green and M. L. H. Green, in *Comprehensive Inorganic Chemistry*, J. C. Bailar, Jr., H. J. Emeleus, R. S. Nyholm, A. F. Trotman-Dickerson, Eds. (Pergamon, Oxford, 1973), vol. 4, p. 355.
9. G. L. Geoffroy and J. R. Lehman, *Adv. Inorg. Chem. Radiochem.* **20**, 189 (1977).
10. H. D. Kaesz and R. B. Saillant, *Chem. Rev.* **72**, 213 (1972).
11. F. A. Cotton and G. Wilkinson, *Advanced Inorganic Chemistry* (Interscience, New York, ed. 3, 1972), pp. 149, 682, and 770.
12. E. L. Muetterties, Ed., *Transition Metal Hydrides* (Dekker, New York, 1971), vol. 1.
13. For a discussion of binary actinide hydrides (such as UH_3, ThH_2, and Th_4H_{15}) see J. J. Katz and G. T. Seaborg, *The Chemistry of the Actinide Elements* (Wiley, New York, 1957), pp. 35 and 133.
14. T. J. Marks, *Prog. Inorg. Chem.*, in press.
15. ———, *Acc. Chem. Res.* **9**, 223 (1976).
16. E. C. Baker, G. W. Halstead, K. N. Raymond, *Struct. Bonding (Berlin)* **25**, 23 (1976).
17. J. M. Manriquez, P. J. Fagan, T. J. Marks, *J. Am. Chem. Soc.* **100**, 3939 (1978).
18. R. Bau, W. E. Carroll, D. W. Hart, R. G. Teller, T. F. Koetzle, *Adv. Chem. Ser.* **167**, 73 (1978).
19. B. A. Frenz and J. A. Ibers, in (*12*), p. 33.
20. A. F. Wells, *Structural Inorganic Chemistry* (Oxford Univ. Press, New York, ed. 4, 1975), p. 1014.
21. R. E. Rundle, C. G. Shull, E. O. Wollan, *Acta Crystallogr.* **5**, 22 (1952).
22. W. H. Zachariasen, *ibid.* **6**, 393 (1953).
23. M. R. Churchill, B. G. DeBoer, F. J. Rotella, *Inorg. Chem.* **15**, 1843 (1976).
24. R. W. Broach, A. J. Schultz, J. M. Williams, G. M. Brown, J. M. Manriquez, P. J. Fagan, T. J. Marks, in preparation.
25. I. Bernal and S. F. Watkins, *Science* **178**, 1282 (1972); S. F. Watkins, N. H. Fischer, I. Bernal, *Proc. Natl. Acad. Sci. U.S.A.* **70**, 2434 (1973).
26. The work at Argonne and Oak Ridge National Laboratories is sponsored by the Division of Basic Energy Sciences of the U.S. Department of Energy (at Oak Ridge, under contract W-7405-ENG-26 with the Union Carbide Corporation). Partial support of these collaborative neutron diffraction studies by the National Science Foundation under grants CHE77-22650 (J.M.W.) and CHE76-84494 A01 (T.J.M.) and by a teacher-scholar fellowship from the Camille and Henry Dreyfus Foundation (T.J.M.) are gratefully acknowledged.

10 August 1978; revised 30 October 1978

Human and Mouse Hypoxanthine-Guanine Phosphoribosyltransferase: Dimers and Tetramers

Abstract. *Human and mouse hypoxanthine-guanine phosphoribosyltransferase subunits combine to form an active heteropolymer. Dimers form the basic subunit structure of the enzymes, yet the dimers can readily associate to form tetramers. The equilibrium between dimers and tetramers is significantly influenced by the ionic strength of the enzyme solvent.*

Hypoxanthine-guanine phosphoribosyltransferase (HGPRT; E.C. 2.4.2.8.), the enzyme that catalyses the conversion of hypoxanthine and guanine to mononucleotides, is specified by mammalian X chromosomes (*1*, *2*). This enzyme has been the principal focus for studies of mutagenesis in mammalian cells (*3*, *4*); yet, neither the subunit structure nor the nature of interspecific subunit interactions have been defined. On the basis of estimates of the molecular weight of the purified enzymes from Chinese hamster, mouse, and human cells, it has been proposed that the enzymes are trimers (*5*). However, studies of interspecific hybrids (*6*) suggest that the enzymes may not be trimers, although these observations have been difficult to evaluate because of the presence of multiple enzyme bands in the parent cells as well as in hybrid cells. The analysis is complicated by the fact that HGPRT can exist in more than one form within a cell, as isoenzymes (*7*). Furthermore, the complexity is compounded by the presence of pseudoisoenzymes resulting from disulfide bond formation (*8*).

We have examined the interaction of the mouse and human enzyme subunits in hybrid cells, using conditions which eliminate pseudoisoenzymes (*8*). Our results indicate that the subunits of human and mouse HGPRT interact to form a single active heteropolymer and that, under the conditions of isoelectric focusing, the enzymes are dimers. Evidence is also presented that the enzyme dimers associate to form tetramers in solvents of high ionic strength.

Our strategy was to select hybrids on the basis of complementation at the thymidine kinase (TK) locus, and to look for those which retain a human X chromosome so that both murine and human forms of HGPRT are present in the hybrid cell. The hybrids were derived from normal human skin fibroblasts and LM (TK^-) Cl-1D, a derivative of the mouse L cell lacking TK but wild type for HGPRT. Fusion was mediated with 50 percent polyethylene glycol (*9*) in saline. Selection for the mouse/human hybrids was carried out in HOT medium [HAT (*3*) containing $10^{-6}M$ ouabain], which eliminates both parental cells. After 5 weeks of selection, hybrid clones were picked with stainless steel cylinders and transferred to individual dishes containing HOT. The clones were then replicate-plated: one petri dish was used for isoelectric focusing of HGPRT, one

0036-8075/79/0112-0174$00.50/0